Catalysis Today 160 (2011) 184–190

Contents lists available at ScienceDirect

Catalysis Today

journal homepage: www.elsevier.com/locate/cattod

Hydrogenation of CO_2 to formic acid on supported ruthenium catalysts

Cuiying Hao, Shengping Wang**, Maoshuai Li, Liqiong Kang, Xinbin Ma*

Key Laboratory for Green Chemical Technology of Ministry of Education, School of Chemical Engineering and Technology, Tianjin University, Weijin Road 92, Nankai District, Tianjin 300072, PR China

ARTICLE INFO

Article history:
Available online 2 July 2010

Keywords:
Supported ruthenium catalyst
Carbon dioxide
Heterogeneous hydrogenation
Formic acid

ABSTRACT

We report on the preparation and application of novel heterogeneous supported ruthenium catalysts. The catalysts are active in the synthesis of formic acid from the hydrogenation of carbon dioxide and are characterized by Fourier transform infrared spectroscopy, X-ray photoelectron spectroscopy, X-ray powder diffraction analysis and transmission electron microscopy. Abundant hydroxyl groups, which interact with the ruthenium components, play an important role in the catalytic reactions. Highly dispersed ruthenium hydroxide species enhance the hydrogenation of CO_2, while crystalline RuO_2 species, which are formed from the relatively high ruthenium content or the pH of the solution during preparation of the catalyst, restrict the production of formic acid. Optimal activity of ruthenium hydroxide as a catalyst for the hydrogenation of CO_2 to formic acid is achieved over a γ-Al_2O_3 supported 2.0 wt% ruthenium catalyst, which is prepared in a solution of pH 12.8 with $NH_3{\cdot}H_2O$ as a titration solvent. A possible hydrogenation mechanism for the hydroxide ruthenium catalyst is proposed.

1. Introduction

Carbon dioxide (CO_2) is a major contributor to the greenhouse effect, and its utilization has been of global interest from both theoretical and practical viewpoints. The utilization and transformation of CO_2 into value-added chemicals have attracted much attention in recent years as requirements for its trapping from power plants [1–3]. Although CO_2 is widely used as a reagent for the synthesis of aspirin and carbonates [4–9], the development of efficient methods of CO_2 reduction is highly desirable. However, CO_2 is extremely thermodynamically stable and requires efficient catalysts or electrical reductive processes for its chemical transformation. As one of the most promising directions for CO_2 fixation, catalytic hydrogenation has shown appreciable efficiency for reactions with optimized conditions and catalysts [10–20].

Formic acid is a fundamental chemical feedstock in the organic chemical industry. It has been used in the perfume industry as a mordant in the dyeing industry, as a neutralizer in tanning, and as a disinfectant and preservative agent in sanitary stations. As a raw material in the chemical industry, it has promoted the production of formate esters which have been used to produce a variety of organic derivatives such as aldehydes, ketones, carboxylic acids and amides. Additionally, formic acid has been considered as a candidate for methanol-alternative fuels in methanol fuel cells, as the direct fuel for electricity generation, and as a fuel for automobiles due to its much better electrochemical oxidation at Pt–Ru/C electrodes [21,22]. Currently, commercial processes for formic acid production are mainly the result of hydrolysis of methyl formate and direct synthesis from carbon monoxide (CO) and water. As these traditional methods consume a large amount of energy and produce hazardous waste, the development of a clean method of formic acid synthesis is a high priority. The hydrogenation of CO_2, as shown in the equation below, provides a possible technique to synthesize formic acid using CO_2 as a raw material [23].

$$CO_2 + H_2 \rightarrow HCOOH$$

The direct synthesis of formic acid from the hydrogenation of CO_2 has been carried out for many decades, and was first reported by Farlow and Adkins in 1935 using Raney nickel as a catalyst under 20–40 MPa and at 353–423 K [24]. A homogeneous Ru- or Pd-complex catalyzed sample was reported under less extreme conditions [25]. The process is thermodynamically unfavorable and the standard Gibbs free energy of this reaction at 298 K is $\sim$32.9 kJ mol^{-1}; acidic alcohols and organic bases with intermediate basicity are usually added to the reaction mixture to extract the formic acid, and this increases the reaction rate by an order of magnitude [26]. Until now, the best known catalytic systems for this process have been based on the metal complexes of the second and third row transition metals of groups VIII to IIB, such as ruthenium and rhodium, which are usually combined with halides or hydrides as anionic ligands and phosphines as neutral ligands. Moreover, reactions in different media, such as organic solvents

* Corresponding author. Tel.: +86 22 27409248; fax: +86 22 87401818.
** Corresponding author. Tel.: +86 22 87401818; fax: +86 22 87401818.
E-mail addresses: spwang@tju.edu.cn (S. Wang), xbma@tju.edu.cn, xinbinma@gmail.com (X. Ma).

0920-5861/$ – see front matter © 2010 Elsevier B.V. All rights reserved.
doi:10.1016/j.cattod.2010.05.034

[27], water [28,29], supercritical CO_2 [30–32], and ionic liquids [33] have shown satisfactory reaction rates [34–38]. Of these media, the highest reaction rate was achieved by using supercritical CO_2 [14].

Although the reasonable conversion and yield of formic acid have been obtained using homogeneous catalysts, separation of formic acid from the bases and catalysts remains a challenge. Therefore, the development of a heterogeneous catalytic system is highly desirable. To the best of our knowledge very few heterogeneous systems with solid (supported) catalysts have been investigated. Ruthenium complex catalysts immobilized on silica and polystyrene resin have been examined [39–41]. A more attractive heterogeneous system is the activated carbon supported ruthenium prepared by conventional impregnation [42]. An advantage of this method is that the use of hazardous and expensive reagents, such as $LiAlH_4$ or $NaBH_4$, can be avoided [43]. In these studies, formic acid is manufactured using an inexpensive hydrogenation catalyst. Moreover, since separation of the catalyst is easy, the manufacture of formic acid is simple and the loss of catalyst is also reduced, although the yield of formic acid is low. Therefore, the search for an efficient heterogeneous catalyst is necessary. In most studies of this process using ruthenium catalysts, ruthenium hydride species were found to be active components in the catalytic cycle [29–38,44]. In the hydrogenation of CO_2 to formic acid with ruthenium complexes under acidic conditions in water, $[Ru{-}OH_2]^{2+}$, which is subsequently hydrogenated to ruthenium hydride species, was suggested as the initial active species for the catalytic cycle [45]. Additionally, a theoretical study of the hydrogenation of CO_2 to formic acid in a potassium hydroxide (KOH) solution indicated that the introduction of strong donor ligand and hydroxyl groups would improve the catalytic efficiency [46]. Therefore, this paper describes the application of heterogeneous ruthenium hydroxide catalysts in hydrogenating CO_2 to create formic acid. The catalysts reported here show considerable activity and high selectivity and can be easily recycled by filtration or centrifugation.

2. Experimental

2.1. Catalyst preparation

MgO with a higher specific surface area than the purchased product was synthesized following the procedures outlined by Di Cosimo and Apesteguía [47]. Activated carbon was treated in a 0.1 mol L^{-1} KOH solution followed by a 0.1 mol L^{-1} HNO_3 solution and washed with deionized water in order to remove the residual ash on the surface. The sample was then dried at 393 K for 24 h and stored in a desiccator. The γ-Al_2O_3 was treated in deionized water for 5 h, followed by drying at 393 K for 24 h. After the impregnation, the dried material was subsequently calcined in an open-air furnace at 823 K for 12 h.

Ruthenium hydroxide catalysts were prepared by modification of the preparation of $Ru(OH)_3$ [48]. 4.0 g γ-Al_2O_3 was vigorously stirred in an aqueous solution of $RuCl_3$ (acquired from Sino-Platinum Metals Co. Ltd., analysis reagent grade) (100 mL, 8.0×10^{-3} mol L^{-1}) for 15 min at room temperature. The pH of the solution was slowly adjusted to a constant value and the resultant slurry was stirred for an additional 24 h. The solid was then separated by filtration and washed with a large amount of deionized water in order to remove the chlorine ions. The resultant solid material was dried at 393 K for 24 h and stored in a desiccator for the following usage.

2.2. Hydrogenation of carbon dioxide to formic acid

Hydrogenation of carbon dioxide to formic acid was carried out in a 100-mL stainless steel autoclave with a magnetic stirrer. In a typical run, 5 mL of triethylamine, 0.1 mmol of ruthenium hydroxide catalyst, and 15 mL of ethanol as solvent were placed in the autoclave, followed by flushing with H_2 three times to remove air. The autoclave was heated by a mantle equipped with a temperature controller to 353 K (unless otherwise specified) ensuring temperature stabilization inside the autoclave. The reactor was then pressurized by H_2 to 5.0 MPa at the required temperature. The mixture was stirred under these conditions for 5 min. Subsequently, CO_2 was introduced from a cooled (−5 °C) reservoir by a high pressure liquid chromatography pump and up to a total pressure of 13.5 MPa, which was considered as the start of the reaction. After the reaction (1 h), the autoclave was cooled in the ice water until the pressure stabilized and then depressurized to ambient conditions. Ethyl acetate (2 mL) was added in the mixture after the reaction as an internal standard for the quantitative analysis of product.

The liquid mixture in the autoclave was analyzed by a Shimadzu GC 8A gas chromatograph equipped with a propack Q column (Shimadzu, 2 m × 3 mm) and a thermal conductivity detector. The yield is expressed as the turnover number (TON) of formic acid, which is the moles of formic acid produced per mole of ruthenium used. The gaseous samples were analyzed using an SP 3420 GC with a TDX-01 column (Tianjin Chromatograph Company, 2.5 m × 3 mm) and a thermal conductivity detector. The gaseous samples collected at the reactor outlet are only CO_2 and H_2 and no other gas products are produced.

2.3. Catalyst characterization

Fourier transform infrared (FTIR) spectroscopic measurements were carried out on a Bruker VECTOR22 spectrometer with the powdered catalysts pressed into a 10 mg cm^{-2} self-supporting wafer. The scanning range was from 500 to 4000 cm^{-1} with a resolution of 4 cm^{-1}.

X-ray photoelectron spectroscopy (XPS) was employed to determine the surface composition and chemical state of the surface ruthenium species. The measurements were made with a Perkin–Elmer PHI 1600 ESCA system with Mg Kα (1253.6 eV) radiation as the excitation source. The sample was fixed to the specimen holder with double-sided adhesive tape. To eliminate the charging effect, calibration of the binding energy was accomplished with respect to the internal standard of the C_{1s} peak (284.5 eV). The spectra were obtained at room temperature under ultrahigh vacuum ($\sim 1.33 \times 10^{-8}$ Pa).

Powder X-ray diffraction crystalline phases were determined at room temperature on a Rigaku C/max-2500 diffractometer equipped with a Cu Kα radiation anode (λ = 1.54056 Å, 40 kV and 200 mA). The intensity of the signal was measured by step scanning over 2θ with a scanning rate of 12° min^{-1} from 2θ = 10–80°.

Transmission electron microscope (TEM) analysis was performed on a Philips Tecnai G2 F20, with the point and linear resolution 0.248 and 0.102 nm, respectively. A small quantity of the as-prepared γ-Al_2O_3 supported 2.0 wt% ruthenium catalyst was dispersed in ethanol and then onto copper grids in order to perform detailed measurements. Energy-dispersive X-ray (EDX) analysis was coupled to TEM observations to determine the surface composition of the catalyst.

3. Results and discussion

3.1. Fourier transform infrared spectroscopy

An FTIR spectrum represents a fingerprint of a sample with absorption peaks that correspond to the vibrational frequencies of the molecular bonds of the material. To determine the presence of hydroxyl groups, and the relationship of catalytic activity and

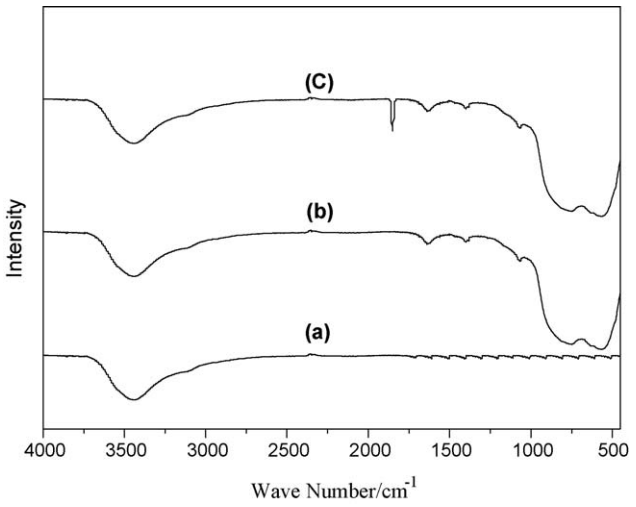

Fig. 1. FTIR spectra of (a) activated carbon, (b) pure γ-Al_2O_3 and (c) γ-Al_2O_3 supported 2.0 wt% ruthenium catalyst.

interaction between the ruthenium component with the hydroxyl groups on the catalyst surfaces, MgO, activated carbon, γ-Al_2O_3 and γ-Al_2O_3 supported 2.0 wt% ruthenium were investigated by FTIR. There are no hydroxyl groups on the MgO surface (not shown). However, as shown in Fig. 1(a), it can be seen that a few broad ν(OH) bands in the range 3100–3700 cm^{-1} attributed to free or quasi-free surface hydroxyl groups are observed on the activated carbon. Similarly, bands in the range 3100–3700 cm^{-1} can also be seen on both pure γ-Al_2O_3 and γ-Al_2O_3 supported 2.0 wt% ruthenium catalyst as shown in Fig. 1(b) and (c). Moreover, strong and broad characteristic bands in the region 500–900 cm^{-1}, which are attributed to the stretching vibrations of a lattice of interlinked (condensed) tetrahedral or vibrational molecules localized on the surface layer and most likely due to the deformation of surface hydroxyl groups, are also found [49]. This indicates that the main species on the surface of pure γ-Al_2O_3 and γ-Al_2O_3 supported ruthenium are hydroxyl groups. A sharp absorption band also appears around 1856 cm^{-1} on the γ-Al_2O_3 supported 2.0 wt% ruthenium catalyst, which indicates the transformation of the surface-bound functional group after the addition of ruthenium. The appearance of a peak at 1856 cm^{-1}, which is attributed to the vibration of ruthenium species, suggests the interaction of hydroxyl groups with the ruthenium component [50]. Therefore, we confirm that hydroxyl groups and Ru–OH species are present on the surface of γ-Al_2O_3 supported 2.0 wt% ruthenium. It is inferred that the hydroxyl groups have interacted with the active ruthenium component to promote the formation of the ruthenium hydroxide species.

3.2. X-ray photoelectron spectroscopy analysis

Spectra of the O_{1s} peaks of γ-Al_2O_3 supported 2.0 wt% ruthenium catalyst are presented in Fig. 2(a), the peak of the catalyst at a binding energy of 531.1 eV is in agreement with the O_{1s} binding energy of the hydroxyl species on the pure γ-Al_2O_3 surface. Moreover, the ruthenium $3p_{3/2}$ peak of $RuCl_3{\cdot}3H_2O$ and γ-Al_2O_3 supported 2.0 wt% ruthenium catalyst is at binding energies of 463.3 and 462.3 eV, respectively, as shown in Fig. 3. It is inferred that the binding energy of Ru^{3+} $3p_{3/2}$ shifting towards a lower value could be caused by the interaction of the active ruthenium components with the species on the γ-Al_2O_3 surface. It is evident that the active ruthenium components interact with the hydroxyl groups on the surface. However, for the γ-Al_2O_3 supported 6.0 wt% ruthenium catalyst, we observed a broad spectrum (Fig. 2(b)). A deconvolution of the spectrum produces two peaks located at binding energies of

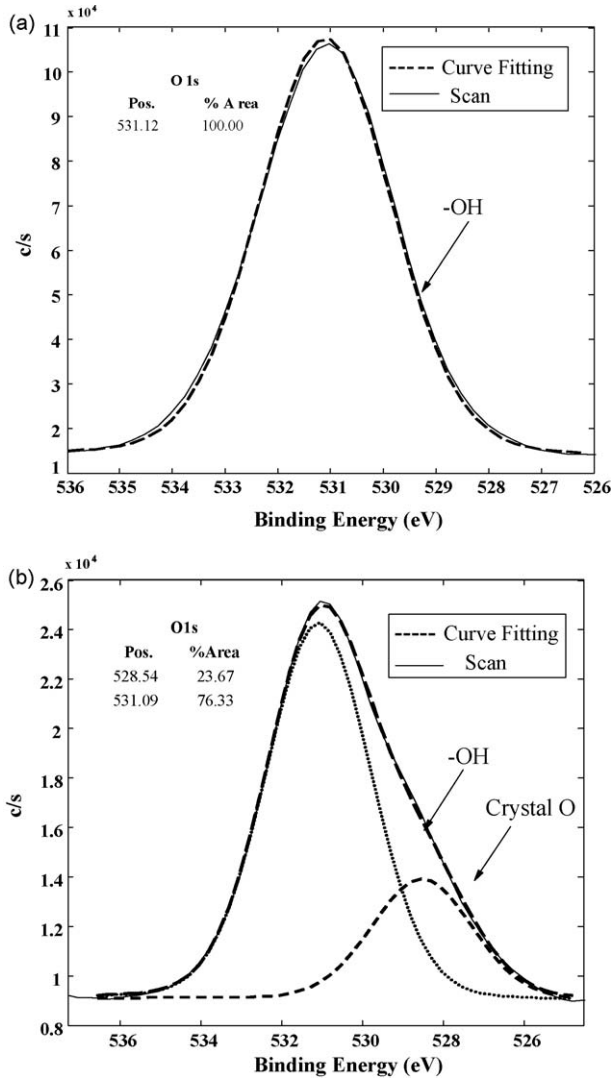

Fig. 2. XPS spectra of the O_{1s} peaks of (a) γ-Al_2O_3 supported 2.0 wt% ruthenium catalyst and (b) 6.0 wt% ruthenium catalyst.

531.1 eV (hydroxyl) and 528.5 eV, respectively. The peak at 528.5 eV is assigned to the crystal [O] species on the surface, which is formed with high ruthenium loading.

3.3. X-ray powder diffraction analysis

XRD patterns of the γ-Al_2O_3 supported ruthenium catalysts with different ruthenium concentrations are shown in Fig. 4(a). For 2 wt% ruthenium, the characteristic peaks at $2\theta = 28.0^\circ$, 35.1°, 40.0° and 54.3° are consistent with those of γ-Al_2O_3, and no feature of crystalline ruthenium dioxide (RuO_2) is observed. This indicates that active ruthenium species are highly dispersed on the γ-Al_2O_3 support material and that the fine interaction occurred between the ruthenium components and γ-Al_2O_3. However, characteristic peaks of crystalline ruthenium dioxide emerged when the ruthenium loading was up to 4.0 wt%. This observation, combined with the results shown in Fig. 3, suggests that the formation of crystalline RuO_2, but not the hydroxide ruthenium species, is more favorable with a relatively high ruthenium loading. It is inferred that the impregnated ruthenium components could interact preferentially with hydroxyl groups on the γ-Al_2O_3 surface and that the redundant ruthenium components would interact with [O] to form crystalline RuO_2, which is in agreement with the XPS results.

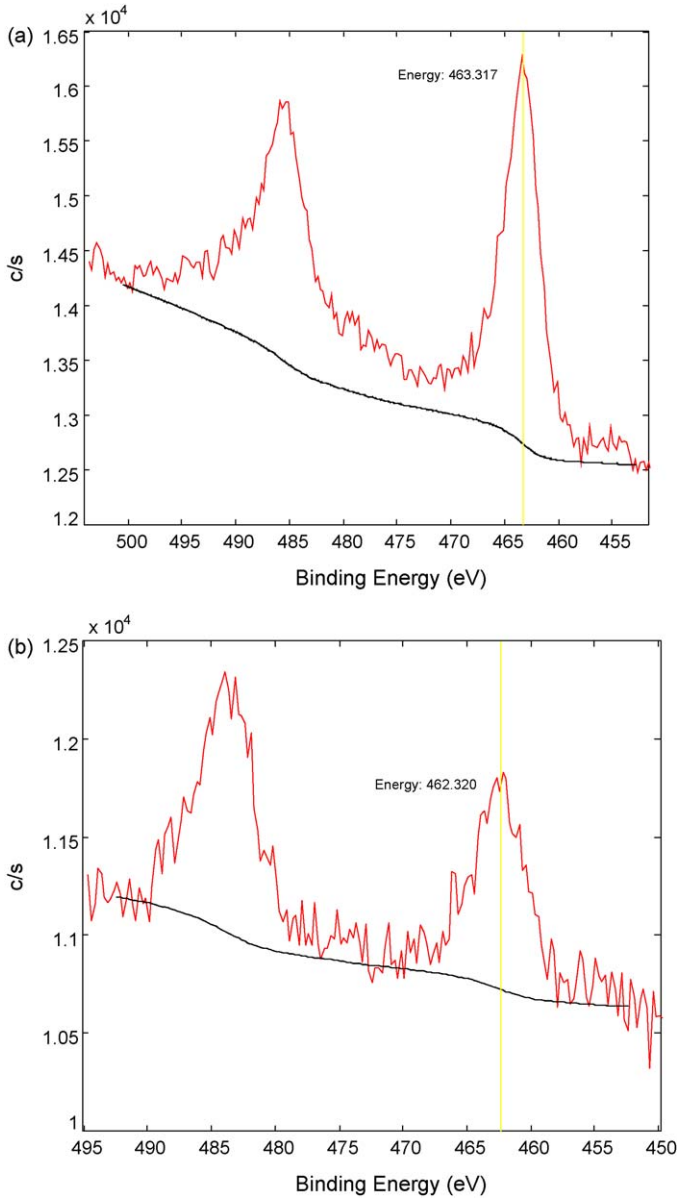

Fig. 3. XPS survey Mg Kα photoelectron spectra of the (a) pure $RuCl_3 \cdot 3H_2O$ and (b) γ-Al_2O_3 supported 2.0 wt% ruthenium catalysts.

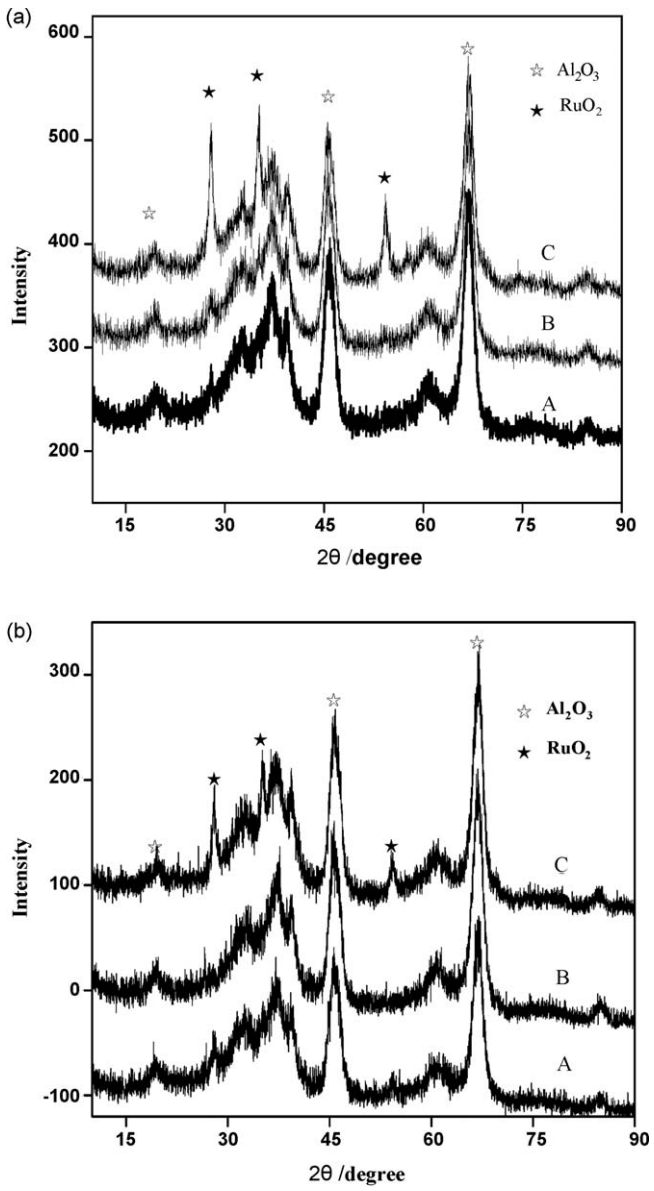

Fig. 4. XRD spectra of (a) γ-Al_2O_3 supported catalyst with different amounts of ruthenium loading. A – 2.0 wt%, B – 4.0 wt%, C – 6.0 wt% and (b) γ-Al_2O_3 supported 2.0 wt% ruthenium catalysts with different pH value of preparation solution. A – PH = 12.8, B – PH = 13, C – PH = 13.2.

The pH of the precursor solution for the supported ruthenium catalyst also affects the structure of ruthenium species on the surface. XRD patterns in Fig. 4(b) were obtained for γ-Al_2O_3 supported ruthenium catalysts prepared with various values of pH. In a low pH solution, characteristic diffraction peaks are nearly the same as those of the γ-Al_2O_3, and no features from either ruthenium metal or RuO_2 are observed. However, characteristic peaks of crystalline RuO_2 appear when the pH of the preparation solution is higher than 13. The relatively high pH of the preparation solution could lead to the formation of crystalline RuO_2 on the surface of the catalyst.

3.4. Transmission electron microscope analysis

Particles of ruthenium metal or RuO_2 were not detected on a γ-Al_2O_3 supported 2.0 wt% ruthenium catalyst by TEM as shown in Fig. 5(a). However, EDX analysis shows that ruthenium, aluminium, copper, oxygen and carbon are present on the surface of the catalyst as shown in Fig. 5(b). These results further reveal that ruthenium hydroxide is highly dispersed in an amorphous form on γ-Al_2O_3 supported 2.0 wt% ruthenium catalyst which, as will be discussed, is favorable for CO_2 hydrogenation to formic acid.

3.5. Performance of hydroxide ruthenium catalysts

3.5.1. Effect of support

The basic role of an appropriate support is to maintain the catalytic active phase in a highly dispersed state. However, it is found that the support may also contribute to the catalytic activity and react with other catalytic components during preparation. In our case, as mentioned earlier, the presence of the base is crucial for favorable thermodynamics, and a stoichiometric amount of base to improve the rate of the hydrogenation of CO_2 to formic acid is usually required. Previous studies indicate that in a supercritical system, the yield of formic acid reaches a high value in the presence of triethylamine (with an optimized pK_a of conjugate acid between 8 and 12), whereas no formic acid is obtained in the absence of a base [1,14,26]. However, after the reaction, the base has to be neu-

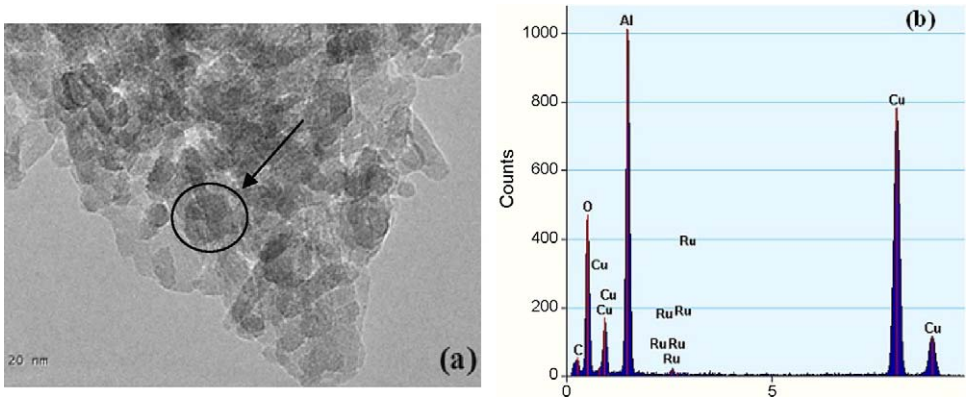

Fig. 5. (a) TEM photographs and (b) EDX analysis of catalytic particle of γ-Al_2O_3 supported 2.0 wt% ruthenium catalyst.

tralized by a strong acid to yield formic acid ($pK_a \sim 3.6$), and the separation of catalysts and organic base is fairly complicated [51]. Therefore, MgO with strong basic sites was used as a support in this study, so that this heterogeneous catalytic system could make the separation of products from catalysts relatively easy. Unfortunately, no formic acid was obtained on the MgO-based ruthenium catalyst as shown in Table 1. The invalidation of MgO as the support might be due to its relatively strong basic characteristic. Active ruthenium species could become inactive in the presence of MgO, which has a very high pH, and are thus incapable of promoting the reaction. As shown in Fig. 4(b) (Curve C), the high pH of the solution causes the formation of crystalline RuO_2 on the surface of the catalyst, leading to poor catalytic activity. On the other hand, no formic acid was formed on MgO, possibly due to the absence of hydroxyl groups on the surface (not shown). Therefore, we have attempted to find a suitable support with abundant hydroxyl groups on the surface.

Activated carbon attracts our attention as a support because it forms oxygen-bonded surface groups, including quinine, carboxyl, and hydroxyl groups [52]. Moreover, the hydroxyl groups on the activated surface facilitate the adsorption of CO_2, and the adsorption capability increases with the increase of the concentration of hydroxyl groups [53]. Therefore, immobilizing more hydroxyl groups on an activated carbon-based ruthenium catalyst may be favorable for the formation of formic acid. As expected, activated carbon supported ruthenium catalyst with few hydroxyl groups as indicated in Fig. 1(a) is active for the hydrogenation of CO_2 to formic acid, which indicates that hydroxyl groups on the surface play an important role in the catalytic reaction. Ten TON of formic acid is obtained under the reaction conditions as listed in Table 1.

γ-Al_2O_3 is another important catalytic material that is frequently used in the automotive and petroleum industries [54]. The most attractive feature of γ-Al_2O_3 is the abundant hydroxyl groups on the surface. The form of these surface hydroxyl groups is quite complex, and this has been determined by means of FTIR and nuclear magnetic resonance spectroscopy [49]. The effect of the γ-Al_2O_3 supported ruthenium catalysts on the catalytic performance is shown in Table 1. The yield of formic acid is much higher with γ-Al_2O_3 as the support compared to activated carbon. This is likely due to the greater number of hydroxyl groups on the surface, which favors the formation of hydroxide ruthenium to promote the hydrogenation of CO_2. Therefore, we chose γ-Al_2O_3 as a support for the preparation of a ruthenium hydroxide catalyst, of which physicochemical properties have been investigated in detail. We have screened the activity of pure activated carbon or γ-Al_2O_3 (i.e., no ruthenium loading), and the results revealed that no formic acid was formed under the same reaction conditions. Therefore, we consider that the ruthenium species, the active species in promoting formic acid formation, can be correlated to their interactions with the hydroxyl groups to form the active hydroxide ruthenium species.

Table 1
Effect of supports on the catalytic performance of catalysts[a] for the hydrogenation of CO_2 to formic acid.[b].

Support	TON of formic acid	Yield of formic acid (mmol)
MgO	0	0
Activated Carbon	10	1.0
Al_2O_3	91	9.1

[a] 0.1 mmol 2.0 wt% Ru catalyst.
[b] Reaction condition: temperature 353 K, 5 MPa of H_2, total pressure 13.5 MPa, 5 mL $N(C_2H_5)_3$, 15 mL EtOH, stirring rate 250 rpm, reaction time 1 h.

3.5.2. *Effect of the titration solvent and pH of the preparation solution*

As mentioned above, the introduction of the strongly donating hydroxyl groups is expected to improve the catalytic performance in the hydrogenation of CO_2 to formic acid in a KOH solution [46]. In order to test this hypothesis and to further verify that the high hydrogenation rate on γ-Al_2O_3 is ascribed to the abundant hydroxyl groups on the surface, $NH_3{\cdot}H_2O$ and NaOH solution were used as the titration solvent to control the pH during preparation of the catalyst. Considering that the dissociation of $NH_3{\cdot}H_2O$ in solution is a process in dynamic equilibrium, self-dissociation was expected to produce more hydroxyl groups to form ruthenium hydroxide than that of sodium hydroxide (NaOH). As expected, the catalyst with $NH_3{\cdot}H_2O$ as the titration solvent is more favorable for the yield of formic acid. The TON of formic acid is increased from 91 to 116 when the pH of the solution is 12.

The influence of pH of the preparation solution from 12 to 13.2 on the performance of γ-Al_2O_3 supported ruthenium catalyst is shown in Fig. 6. The TON of formic acid first increases with the increase of pH of the solution and thereafter sharply decreases when the pH increases. The results suggest that the base titration is required for the effective loading of the active component to prepare the highly active ruthenium hydroxide catalyst. Low pH was unfavorable for the interaction of ruthenium with hydroxyl groups on γ-Al_2O_3, leading to the decrease of reactivity. The optimal TON of formic acid of 139 was observed over the γ-Al_2O_3 supported ruthenium catalyst prepared at a pH of 12.8, and the TON decreased to 91 and 32 at a pH of 13 and 13.2, respectively. The appearance of crystalline RuO_2 on the catalyst prepared in the solution with pH 13.2, as shown in Fig. 4(b) (curve C), suggests that the higher pH of the preparation solution is unfavorable. In addition, the catalyst prepared in the solution with pH 13 possible has caused a small amount of RuO_2 and results in the negligible signals in XRD charac-

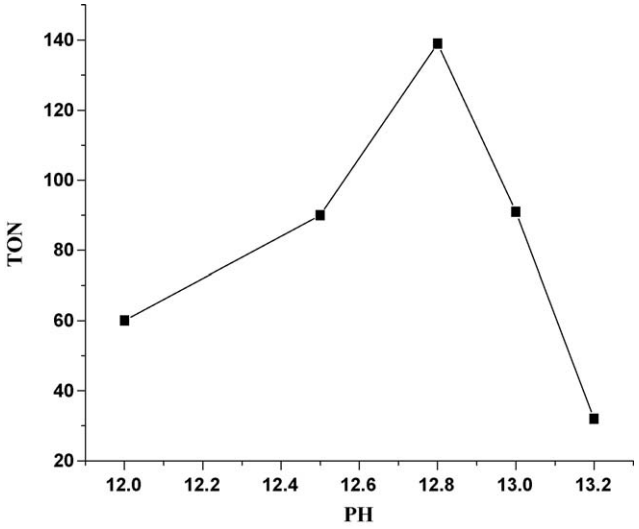

Fig. 6. Effect of pH value of catalyst preparation solution on the catalytic performance for the hydrogenation of CO_2 to formic acid. Conditions: 0.1 mmol Ru/Al_2O_3 catalyst, 5 MPa of H_2, total pressure 13.5 MPa, 5 mL $N(C_2H_5)_3$, 15 mL EtOH, stirring rate 250 rpm, reaction time 1 h.

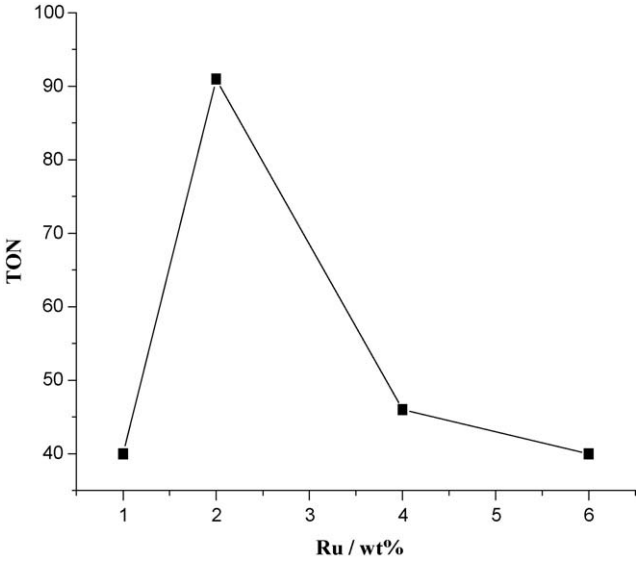

Fig. 7. Effect of ruthenium loading on the catalytic performance for the hydrogenation of CO_2 to formic acid. Conditions: 0.1 mmol Ru/Al_2O_3 catalyst, 5 MPa of H_2, total pressure 13.5 MPa, 5 mL $N(C_2H_5)_3$, 15 mL EtOH, stirring rate 250 rpm, reaction time 1 h.

terization. However, this catalyst has started inducing the decrease of reactivity as shown in Fig. 6.

3.5.3. Effect of ruthenium loading

Fig. 7 shows the influence of ruthenium loading on the catalytic performance of the γ-Al_2O_3 supported ruthenium catalysts of 1.0–6.0 wt%. The TON of formic acid increases gradually with the increase of the ruthenium loading, followed by a steep decrease after 2.0 wt% ruthenium. Therefore, 2.0 wt% was considered to be the optimized ruthenium loading for the hydrogenation of CO_2, resulting in 90 TON of formic acid. A low ruthenium loading with fewer active sites is not sufficient for the effective hydrogenation of CO_2 to formic acid, and a negative effect was observed when the ruthenium loading was beyond a critical value. Crystalline RuO_2 species are formed when the ruthenium loading is above 2.0 wt%, further suggesting that the finely dispersed ruthenium species on the γ-Al_2O_3 surface are active species which yield formic acid.

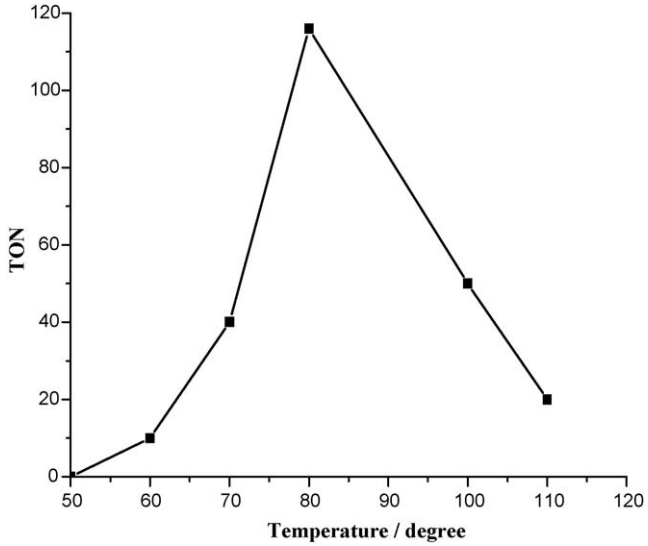

Fig. 8. Effect of reaction temperature on the catalytic performance for the hydrogenation of CO_2 to formic acid. Conditions: 0.1 mmol 2.0 wt% Ru/Al_2O_3 catalyst, 5 MPa of H_2, total pressure 13.5 MPa, 5 mL $N(C_2H_5)_3$, 15 mL EtOH, stirring rate 250 rpm, reaction time 1 h.

3.5.4. Effect of reaction temperature

The influence of reaction temperature, ranging from 50 to 100 °C, on the performance of the γ-Al_2O_3 supported ruthenium catalyst is shown in Fig. 8. The optimal TON of formic acid was observed at 80 °C. At temperatures lower than 80 °C, the yields are low because the chemical adsorption and activation of reactants are unfavorable at low temperatures. With higher temperatures, the average kinetic energy of the reactants increases and the diffusion barrier is overcome. The reaction rate decreases as the temperature increases above 80 °C; for example, the TON of formic acid is 20 at 100 °C. This could be due to the reduced solvability of H_2 in CO_2. We also note that hydrogenation of CO_2, which forms formic acid, is an exothermic reaction, which is unfavorable at high temperature.

3.6. A plausible catalytic scheme

Based on theoretical and experimental studies [29–38,55], divalent transition metal species are the active components in the catalytic cycle. In the case of ruthenium complex, insertion of CO_2 to the metal hydride to generate a metal formate complex or a metal carboxylic acid is always considered as the rate-determined step. Moreover, in the presence of ruthenium complexes under acidic conditions in water, $[Ru{-}OH_2]^{2+}$ is suggested as the initial concentration of the ruthenium–water complex, which is subsequently hydrogenated to the ruthenium hydride species. According to the above results and discussion in this paper, it is obvious that the presence of hydroxyl groups on the catalysts is enormously important for the formation of formic acid. Thus, a plausible catalytic scheme for the hydrogenation of CO_2 to formic acid over hydroxide ruthenium catalyst was proposed, as described in Scheme 1. The Ru–OH species 1 is considered as the initial active ruthenium species of the γ-Al_2O_3 supported ruthenium catalyst. It is subsequently hydrogenated to the ruthenium hydride species 2 (partially based on our observation that high yield could be obtained if H_2 is firstly injected and retained for 30 min in the reactor). Then, CO_2 is inserted into the ruthenium hydride bond to generate the metal formate complex 3. Simultaneously, the formic acid is observed and

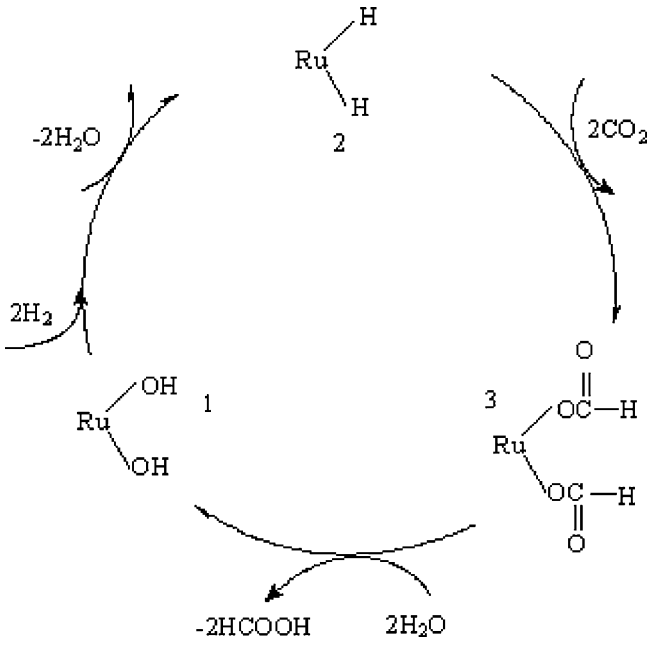

Scheme 1. A plausible catalytic scheme of hydrogenation for the CO_2 on the hydroxide ruthenium catalyst.

the Ru–OH is regenerated as the initial active species for the next catalytic cycle.

4. Conclusion

The chemical properties of heterogeneous ruthenium-based catalysts were investigated by FTIR, XPS, XRD and TEM and the results show that the hydroxide–ruthenium species was formed from the interaction of ruthenium and hydroxyl groups. The effects of experimental variables have been investigated and the optimized conditions include 2.0 wt% ruthenium loading, pH 12.8, $NH_3{\cdot}H_2O$ as a titration solvent, reaction temperature 80 °C, stirring rate 300 rpm, and total pressure 13.5 MPa with H_2 pressure 5 MPa. It has been shown that the interaction between active ruthenium components with hydroxyl groups through formation of Ru–OH species as the active species is crucial for the reaction. Formation of crystalline RuO_2 species at high ruthenium loading and pH of the catalyst leads to lower catalytic activity.

Acknowledgements

Financial support from the Program of Introducing Talents of Discipline to Universities (Grant No. B06006) and the Program for New Century Excellent Talents in University (NCET-04-0242) are gratefully acknowledged.

References

[1] I. Omae, Catal. Today 115 (2006) 33.
[2] J.S. Chang, V.P. Vislovskiy, M.S. Park, Green Chem. 5 (2003) 587.
[3] M.R. Christopher, Org. Process Res. Dev. 11 (2007) 121.
[4] A. Ion, C.V. Doorslaer, V. Parvulescu, Green Chem. 10 (2008) 111.
[5] J. Bian, M. Xiao, S.J. Wang, X.J. Wang, Chem. Eng. J 147 (2009) 287.
[6] J. George, Y. Patel, S.M. Pillai, P. Munshi, J. Mol. Catal. A: Chem. 304 (2009) 1.
[7] G.A. Luinstra, Polym. Rev. 48 (2008) 192.
[8] J.M. Sun, S. Fujita, M. Arai, J. Organomet. Chem. 690 (2005) 3490.
[9] M.H. Chisholm, Z.P. Zhou, J. Am. Chem. Soc. 126 (2004) 11030.
[10] P.G. Jessop, T. Ikariya, R. Noyori, Chem. Rev. 95 (1995) 259.
[11] W. Leitner, Angew Chem. Int. Ed. 34 (1995) 2207.
[12] A.A. Shaikh, S. Sivaram, Chem. Rev. 96 (1996) 951.
[13] X. Yin, J.R. Moss, Coord. Chem. Rev. 181 (1999) 27.
[14] P.G. Jessop, F. Joó, C.C. Tai, Coord. Chem. Rev. 248 (2004) 2425.
[15] K.M.K. Yu, C.M.Y. Yeung, S.C. Tsang, J. Am. Chem. Soc. 129 (2007) 6360.
[16] R. Ghosh, S. Maiti, J. Catal. 264 (2009) 1.
[17] S.C. Lee, J.S. Kim, W.C. Shin, M.J. Choi, S.J. Choung, J. Mol. Catal. A: Chem. 301 (2009) 98.
[18] R.A. Brown, P. Pollet, E. McKoon, J. Am. Chem. Soc. 123 (2001) 1254.
[19] M.J. Burk, S.G. Feng, M.F. Gross, J. Am. Chem. Soc. 117 (1995) 8277.
[20] J.C. Tsai, K.M. Nicholas, J. Am. Chem. Soc. 114 (1992) 5117.
[21] J.Z. Zhang, Z. Li, H. Wang, J. Mol. Catal. A: Chem. 112 (1996) 9.
[22] K.J. Jeong, C.M. Miesse, J.H. Choi, J. Power Sources 168 (2007) 119.
[23] K.R. Stephen, Chem. Eng. News 85 (2007) 11.
[24] M.W. Farlow, H. Adkins, J. Am. Chem. Soc. 57 (1935) 2222.
[25] A. Behr, P. Ebbinghaus, F. Naendrup, Chem. Eng. Technol. 27 (2004) 495.
[26] P. Munshi, A.D. Main, J. Linehan, J. Am. Chem. Soc. 124 (2002) 7963.
[27] Y. Gao, J.K. Kuncheria, H.A. Jenkins, R.J. Puddephatt, G.P. Yap, J. Chem. Soc. Dalton Trans. 18 (2000) 3212.
[28] R. Tanaka, M. Yamashita, K. Nozaki, J. Am. Chem. Soc. 131 (2009) 14168.
[29] J.E. Nádasdi, L.G. Papp, G. Laurenczy, F. Joó, Appl. Catal. A: 255 (2003) 59.
[30] P.G. Jessop, T. Ikariya, R. Noyori, Nature 368 (1994) 231.
[31] P.G. Jessop, P. Hsiao, T. Ikariya, R. Noyori, J. Am. Chem. Soc. 118 (1996) 344.
[32] R. Fornika, H. Gkrls, B. Seemann, W.J.J. Leitner, Chem. Soc. Chem. Commun. (1995) 1479.
[33] Z.F. Zhang, Y. Xie, W.J. Li, Angew Chem. Int. Ed. 47 (2008) 1127.
[34] D.H. Gibson, Chem. Rev. 96 (1996) 2063.
[35] Y.P. Zhang, J.H. Fei, Y.M. Yu, Acta Chim. Sin. 65 (2007) 289.
[36] S.M. Ng, C.Q. Yin, C.H. Yeung, Eur. J. Inorg. Chem. (2004) 1788.
[37] Y. Himeda, N. Onozawa-Komatsuzaki, H. Sugihara, K. Kasuga, J. Am. Chem. Soc. 127 (2005) 13118.
[38] Y.P. Zhang, J.H. Fei, Y.M. Yu, X.-M. Zheng, Acta. Chim. Sin. 64 (2006) 845.
[39] A. Baiker, Appl. Organ. Chem. 14 (2000) 751.
[40] Y.P. Zhang, J.H. Fei, Y.M. Yu, Catal. Commun. 5 (2004) 643.
[41] Y.M. Yu, J.H. Fei, Y.P. Zhang, Chin. Chem. Lett. 17 (2006) 261.
[42] Maruzen Petrochem Co. Ltd., JP 2001288137-A, April 03, 2000.
[43] E. Albert, F. Eugene, C. Jacobson, Notes (1952) 943.
[44] Y. Musashi, S. Sakaki, J. Am. Chem. Soc. 122 (2000) 3867.
[45] S. Ogo, R. Kabe, H. Hayashi, Dalton Trans. (2006) 4657.
[46] Y. Ohnishi, T. Matsunaga, Y. Nakao, H. Sato, S. Sakaki, J. Am. Chem. Soc. 127 (2005) 4021.
[47] J.I. Di Cosimo, C.R. Apesteguía, J. Mol. Catal. A: Chem. 130 (1998) 177.
[48] K. Yamaguchi, N. Mizuno, Angew Chem. 114 (2002) 4720.
[49] C. Morterra, G. Magnacca, Catal. Today 27 (1996) 497.
[50] M.L. Man, Z.Y. Zhou, S.M. Ng, Dalton Trans. 19 (2003) 3727.
[51] H. Hideki, S. Ogo, S. Fukuzumi, Chem. Commun. 27 (2004) 2714.
[52] F. Rodríguez-reinoso, Carbon 36 (1998) 159.
[53] L.D. Zhang, X.N. Wang, C.Y. Han, J. Peiking, Univ. Chem. Technol. 34 (2007) 76 (in Chinese).
[54] M. Trueba, S.P. Trasatti, Eur. J. Inorg. Chem. (2005) 3393.
[55] D.Y. Hwang, A.M. Mebel, J. Phys. Chem. A 108 (2004) 10.